

Research Article

Analytical Solution for One-Dimensional Transport of Particles considering Dispersion in Deposition Kinetics

Xingxin Chen ¹, Xinran Zhang,¹ and Zhonghan Wu²

¹School of Civil Engineering, Huaqiao University, Xiamen, Fujian Province 361021, China

²School of Civil Engineering, Beijing Jiaotong University, Beijing 100044, China

Correspondence should be addressed to Xingxin Chen; chenxx@hqu.edu.cn

Received 3 December 2018; Revised 24 January 2019; Accepted 12 February 2019; Published 19 March 2019

Academic Editor: Zhenjiang You

Copyright © 2019 Xingxin Chen et al. This is an open access article distributed under the Creative Commons Attribution License, which permits unrestricted use, distribution, and reproduction in any medium, provided the original work is properly cited.

The study of particle transport in porous media is of great significance for pollution mitigation, grouting reinforcement, municipal solid waste landfill management, and groundwater exploitation. We developed an analytical solution for a corrected convection-dispersion model that takes into account the effects of dispersion on deposition kinetics with regard to the particle concentration decay type. The rationality and correctness of the solution were verified using time, distance, deposition coefficient, diffusion coefficient, and decay coefficient. As the time increased, the particle concentration increased from zero to the peak value, then decreased to zero. However, as distance increased, the peak value of particle concentration gradually decreased. The deposition coefficient affected the magnitude of the peak value and the distance corresponding to the peak value. In addition, the greater the attenuation coefficient, the smaller the peak value. Overall, our method's prediction results showed that considering the effect of dispersion on deposition kinetics produces better results than when this is not considered.

1. Introduction

Rapid global socioeconomic development is increasing groundwater pollution, which has a serious impact on human lives and productivity. As underground aquifers have complex structures and groundwater flow rates tend to be slow, groundwater pollution is difficult to find and mitigate. It was previously thought that pollutants in aquifers could only be transported via liquids and gases, but it is now understood that pollutants can be adsorbed by small particles carried in water; thus, the presence of such particles promotes the diffusion of pollutants [1–3]. Biological particles (e.g., bacteria, protozoa, and viruses) in aquifers can affect water safety and human health; these are primarily sourced from septic tanks, underground pipeline leaks, sewage leakage, and sludge [4–6]. Thus, the study of particle transport characteristics in porous media is very important for human and ecological health.

The conventional particle transportation model has obtained many analytical solutions regarding the direct prediction and inverse problems [7–13], in which the particle

flux in porous media is the sum of advective and dispersive fluxes. Nevertheless, this model only considers hydrodynamic particle dispersion in the mass balance equation but does not consider the effect of dispersive flux on retention kinetics. Laboratory tests can provide useful context for the ways in which this model's deficiencies make prediction results inaccurate [14]. Increasing numbers of experimental studies [12] show that when conditions are not conducive to adsorption, particle deposition along the depth profile appears in a superexponential form, different from the prediction results of the conventional model. In pulse-injected tracers or suspension to the porous medium, conventional model results suggest that the maximum value of the pulse velocity is the same as that of the flow rate and that the concentration curve is symmetrically distributed on both sides of the maximum. However, many test results [13] show that the first half of the concentration distribution is much larger than the second half and that the transport of the maximum concentration is far less than the flow rate.

Previous research contains a general framework for solutions to solute transport problems subject to time-dependent

boundary conditions that is useful for many applications in science and engineering [15]. However, in this framework, the initial moment of the porous medium is clean (far from the actual situation), limiting its practical and accurate use. In this paper, we present an analytical solution for corrected convection-dispersion models that take into account the effects of dispersion on deposition kinetics and the initial particle concentration, obtained for particle concentration decay types. The solutions were verified using time, distance, deposition coefficient, diffusion coefficient, and decay coefficient [3, 5, 11]. This method is useful for providing benchmarks for complex transport processes, conducting sensitivity analyses of various parameters for particle transport, and estimating parameters for laboratory experiments. Therefore, our results can be widely applied to the treatment of pollutants, grouting reinforcement, municipal solid waste landfill management, and groundwater exploitation.

2. Materials and Methods

2.1. Assumptions

- (1) The porous medium is saturated, homogeneous, and isotropic
- (2) The study area is a semi-infinite porous medium
- (3) The flow is a one-dimensional steady flow, and the convection and dispersion of the particles are also one-dimensional
- (4) The deposition of particles is irreversible, and the release of deposited particles is neglected

2.2. Mathematical Model. Under one-dimensional steady flow conditions, the mass balance equation for particle transport is [10–16]

$$\frac{\partial C}{\partial t} = D \frac{\partial^2 C}{\partial x^2} - u \frac{\partial C}{\partial x} - \frac{\rho}{\phi} \frac{\partial \sigma}{\partial t}, \quad (1)$$

where C is the particle concentration in seepage (ML^{-3}), ϕ is the porosity, D is the diffusion coefficient (L^2T^{-1}), u is the average flow rate in the pore space between the cross sections (LT^{-1}), t is the transport time (T), x is the transport distance (L), ρ is the particle density (ML^{-3}), and σ is the ratio of particle volume deposit on the particle surface to solid medium volume (dimensionless). The deposition kinetic equation that takes into account dispersion [14, 16, 17] gives

$$\frac{\rho}{\phi} \frac{\partial \sigma}{\partial t} = k_{\text{dep}} \cdot C - k_{\text{dep}} \cdot \frac{D}{u} \cdot \frac{\partial C}{\partial x}, \quad (2)$$

where k_{dep} is the deposition coefficient (T^{-1}). Assuming that the dispersivity $D = \alpha_D \cdot u$, substitution of equation (2) into equation (1) gives

$$\frac{\partial C}{\partial t} = D \cdot \frac{\partial^2 C}{\partial X^2} + (D_1 - u) \frac{\partial C}{\partial X} - k_{\text{dep}} \cdot C, \quad (3)$$

where α_D is the longitudinal dispersivity (L). D_1 are coefficients given by

$$D_1 = k_{\text{dep}} \cdot \frac{D}{u}. \quad (4)$$

For decay concentration injection, the initial state and boundary conditions are

$$C(x, 0) = C_i, \quad 0 \leq x < +\infty, \quad (5)$$

$$C(0, t) = C_0 \exp(-\alpha' t), \quad (6)$$

$$\frac{\partial C(\infty, t)}{\partial x} = 0, \quad (7)$$

where C_i is the initial constant concentration in the porous media (M/L), C_0 is the initial injection concentration (ML^{-3}), and α' is the decay coefficient (T^{-1}).

2.3. Solving the Model. Laplace transformation of t for equation (3) on both sides and substitution of the initial condition (5) are obtained by

$$\frac{\partial^2 \bar{C}}{\partial X^2} + \left(\frac{D_1}{D} - \frac{u}{D} \right) \frac{\partial \bar{C}}{\partial X} - \frac{k_{\text{dep}} + s}{D} \bar{C} = -\frac{C_i}{D}, \quad (8)$$

where s is a complex variable corresponding to t and \bar{C} is the Laplace transformation of C .

The solution to equation (8) can be obtained by

$$\begin{aligned} \bar{C} = & C_1 \cdot \exp \left\{ \left(\frac{u}{2D} - \frac{D_1}{2D} \right) x + x \left[\left(\frac{D_1}{2D} - \frac{u}{2D} \right)^2 + \frac{k_{\text{dep}} + s}{D} \right]^{1/2} \right\} \\ & + C_2 \cdot \exp \left\{ \left(\frac{u}{2D} - \frac{D_1}{2D} \right) x - x \left[\left(\frac{D_1}{2D} - \frac{u}{2D} \right)^2 + \frac{k_{\text{dep}} + s}{D} \right]^{1/2} \right\} \\ & - \frac{C_i}{Dk_1 k_2}. \end{aligned} \quad (9)$$

From the boundary conditions of equations (6) and (7), the values of C_1 and C_2 can be obtained; thus,

$$\bar{C} = \left[\frac{C_0}{p + \alpha'} - \frac{C_i}{p + k_{\text{dep}}} \right] \cdot \exp \left\{ \left(\frac{u}{2D} - \frac{D_1}{2D} \right) x - x \left[\left(\frac{D_1}{2D} - \frac{u}{2D} \right)^2 + \frac{k_{\text{dep}} + p}{D} \right]^{1/2} \right\} + \frac{C_i}{p + k_{\text{dep}}}, \quad (10)$$

where p is a complex variable corresponding to t in equations (6) and (7). Assuming that

$$I_1 = \frac{C_0}{p + \alpha'} \cdot \exp \left\{ \left(\frac{u}{2D} - \frac{D_1}{2D} \right) x - x \left[\left(\frac{D_1 - u}{2D} \right)^2 + \frac{k_{\text{dep}} + p}{D} \right]^{1/2} \right\}, \quad (11)$$

$$I_2 = -\frac{C_i}{p + k_{\text{dep}}} \cdot \exp \left\{ \left(\frac{u}{2D} - \frac{D_1}{2D} \right) x - x \left[\left(\frac{D_1 - u}{2D} \right)^2 + \frac{k_{\text{dep}} + p}{D} \right]^{1/2} \right\}, \quad (12)$$

$$I_3 = \frac{C_i}{k_{\text{dep}} + p}, \quad (13)$$

by first letting $\alpha = ((D_1 - u)^2/4D) + k_{\text{dep}} - \alpha'$, $k = D$, in equation (19) of Carslaw and Jaeger [18] and then using $a = -(D_1 - u)^2/4D - k_{\text{dep}}$ in equation (29.2.12) of Abramowitz and Stegun [19], the inverse Laplace transformation of the first term in equation (11) is

$$\begin{aligned} L^{-1}[I_1] &= \frac{C_0}{2} \cdot \exp \left[\left(\frac{u}{2D} - \frac{D_1}{2D} \right) x - \alpha' t \right] \\ &\cdot \left\{ \exp \left[-x \sqrt{\frac{(D_1 - u)^2}{4D^2} + \frac{k_{\text{dep}} - \alpha'}{D}} \right] \right. \\ &\cdot \operatorname{erfc} \left[\frac{x}{2\sqrt{Dt}} - \sqrt{\frac{(D_1 - u)^2}{4D} t + k_{\text{dep}} t - \alpha' t} \right] \\ &+ \exp \left[x \sqrt{\frac{(D_1 - u)^2}{4D^2} + \frac{k_{\text{dep}} - \alpha'}{D}} \right] \\ &\cdot \operatorname{erfc} \left[\frac{x}{2\sqrt{Dt}} + \sqrt{\frac{(D_1 - u)^2}{4D} t + k_{\text{dep}} t - \alpha' t} \right] \left. \right\}. \end{aligned} \quad (14)$$

Hence, the result of the inverse Laplace transformation of the second term in equation (12) is given by

$$\begin{aligned} L^{-1}[I_2] &= -\frac{C_i}{2} \cdot \exp \left[\left(\frac{u}{2D} - \frac{D_1}{2D} \right) x - k_{\text{dep}} t \right] \left\{ \exp \left(-x \frac{|D_1 - u|}{2D} \right) \right. \\ &\cdot \operatorname{erfc} \left(\frac{x}{2\sqrt{D \cdot t}} - \sqrt{\frac{(D_1 - u)^2 t}{4D}} \right) + \exp \left(x \frac{|D_1 - u|}{2D} \right) \\ &\cdot \operatorname{erfc} \left(\frac{x}{2\sqrt{D \cdot t}} + \sqrt{\frac{(D_1 - u)^2 t}{4D}} \right) \left. \right\}. \end{aligned} \quad (15)$$

The result of the inverse Laplace transformation of the second term in equation (13) is given by

$$L^{-1}[I_4] = C_i \cdot e^{-k_{\text{dep}} t}. \quad (16)$$

The inverse transformation of equation (3), which is the solution to the present problem, is thus

$$\begin{aligned} C(x, t) &= \frac{C_0}{2} \cdot \exp \left[\left(\frac{u}{2D} - \frac{D_1}{2D} \right) x - \alpha' t \right] \\ &\cdot \left\{ \exp \left[-x \sqrt{\frac{(D_1 - u)^2}{4D^2} + \frac{k_{\text{dep}} - \alpha'}{D}} \right] \right. \\ &\cdot \operatorname{erfc} \left[\frac{x}{2\sqrt{Dt}} - \sqrt{\frac{(D_1 - u)^2}{4D} t + k_{\text{dep}} t - \alpha' t} \right] \\ &+ \exp \left[x \sqrt{\frac{(D_1 - u)^2}{4D^2} + \frac{k_{\text{dep}} - \alpha'}{D}} \right] \\ &\cdot \operatorname{erfc} \left[\frac{x}{2\sqrt{Dt}} + \sqrt{\frac{(D_1 - u)^2}{4D} t + k_{\text{dep}} t - \alpha' t} \right] \left. \right\} \\ &- \frac{C_i}{2} \cdot \exp \left[\left(\frac{u}{2D} - \frac{D_1}{2D} \right) x - k_{\text{dep}} t \right] \\ &\cdot \left\{ \exp \left(-x \frac{|D_1 - u|}{2D} \right) \cdot \operatorname{erfc} \left(\frac{x}{2\sqrt{D \cdot t}} - \sqrt{\frac{(D_1 - u)^2 t}{4D}} \right) \right. \\ &+ \exp \left(x \frac{|D_1 - u|}{2D} \right) \cdot \operatorname{erfc} \left(\frac{x}{2\sqrt{D \cdot t}} + \sqrt{\frac{(D_1 - u)^2 t}{4D}} \right) \left. \right\} \\ &+ C_i \cdot e^{-k_{\text{dep}} t}. \end{aligned} \quad (17)$$

By letting $C_i = 0$, equation (17) is reduced to the following form:

$$\begin{aligned} C(x, t) &= \frac{C_0}{2} \cdot \exp \left[\left(\frac{u}{2D} - \frac{D_1}{2D} \right) x - \alpha' t \right] \\ &\cdot \left\{ \exp \left[-x \sqrt{\frac{(D_1 - u)^2}{4D^2} + \frac{k_{\text{dep}} - \alpha'}{D}} \right] \right. \\ &\cdot \operatorname{erfc} \left[\frac{x}{2\sqrt{Dt}} - \sqrt{\frac{(D_1 - u)^2}{4D} t + k_{\text{dep}} t - \alpha' t} \right] \\ &+ \exp \left[x \sqrt{\frac{(D_1 - u)^2}{4D^2} + \frac{k_{\text{dep}} - \alpha'}{D}} \right] \\ &\cdot \operatorname{erfc} \left[\frac{x}{2\sqrt{Dt}} + \sqrt{\frac{(D_1 - u)^2}{4D} t + k_{\text{dep}} t - \alpha' t} \right] \left. \right\}. \end{aligned} \quad (18)$$

The analytical solution of the conventional convection-dispersion model, in which the influence of the dispersion on the deposition kinetics is not considered, can be obtained by letting $C_i = 0$ and $D_1 = 0$ in equation (17), delivering the following result:

$$C(x, t) = \frac{C_0}{2} \cdot \exp\left[\frac{ux}{2D} - \alpha't\right] \cdot \left\{ \exp\left[-x\sqrt{\frac{u^2}{4D^2} + \frac{k_{\text{dep}} - \alpha'}{D}}\right] \cdot \text{erfc}\left[\frac{x}{2\sqrt{Dt}} - \sqrt{\frac{u^2}{4D}t + k_{\text{dep}}t - \alpha't}\right] + \exp\left[x\sqrt{\frac{u^2}{4D^2} + \frac{k_{\text{dep}} - \alpha'}{D}}\right] \cdot \text{erfc}\left[\frac{x}{2\sqrt{Dt}} + \sqrt{\frac{u^2}{4D}t + k_{\text{dep}}t - \alpha't}\right] \right\}. \quad (19)$$

3. Results and Discussion

3.1. Calculation Examples. We assessed the analytical solutions in terms of time, distance, dispersion coefficient, deposition coefficient, and attenuation coefficient, using model parameters selected from previous studies [20–23]. Figure 1 shows the relationship between particle concentration and time for various distances predicted by equations (18) and (19) using the parameters given in Table 1. Figure 2 shows the relationship between particle concentration and distance for various times predicted by equations (18) and (19) using the parameters given in Table 1.

Figure 1 shows that particle concentration increases from zero to peak concentration very quickly, then decreases back to zero over a longer time period. In other words, the time required for a concentration increase is far less than that required for a concentration decrease and the peak concentration value gradually decreases with increasing distance. In addition, the prediction results from equation (18) are consistently lower than those from equation (19). Figure 2 shows that the particle concentration gradually decreases with increasing distance, while the greater the time, the smaller the concentration at the same distance. The prediction results from both equations (18) and (19) are very close. Overall, neglecting dispersion in the deposition kinetic equation can result in larger errors in the relationship between particle concentration and time.

Figure 3 shows the relationship between particle concentration and time for two dispersion coefficients predicted by equation (18) using the parameters given in Table 2. Figure 4 shows the relationship between particle concentration and distance for the same two dispersion coefficients using the parameters given in Table 3.

As the influence of the dispersion coefficient on the concentration curve is small, only two dispersion coefficients were tested in Figures 3 and 4. Particle concentration rapidly peaked with increasing time, then gradually decreased to zero; the dispersion coefficients had little influence on

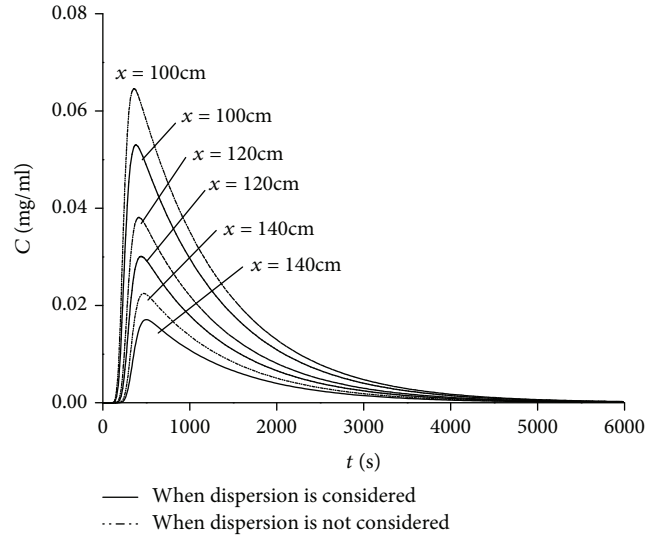


FIGURE 1: Relationship between particle concentration and time for various distances predicted by equations (18) (solid curves) and (19) (dashed curves), using parameters given in Table 1.

TABLE 1: Model parameters used for simulations shown in Figures 1 and 2.

k_{dep} (s^{-1})	D (cm^2/s)	u (cm/s)	C_0 (mg/ml)	α' (s^{-1})
0.01	1	0.36	1	0.001

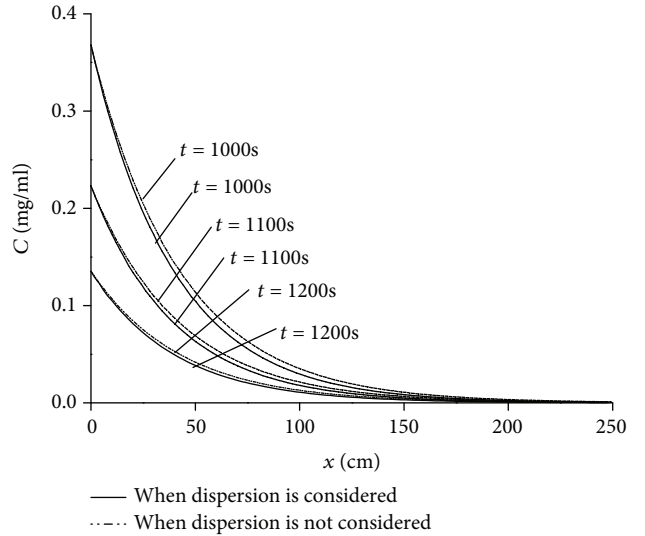


FIGURE 2: Relationship between particle concentration and distance for various times predicted by equations (18) (solid curves) and (19) (dashed curves), using parameters given in Table 1.

particle concentration. Particle concentration decreased with increasing distance; again, the dispersion coefficients had little influence.

Figure 5 shows the relationship between particle concentration and time for four deposition coefficients predicted by equation (18) using the parameters given in Table 4. Figure 6 shows the relationship between particle concentration and

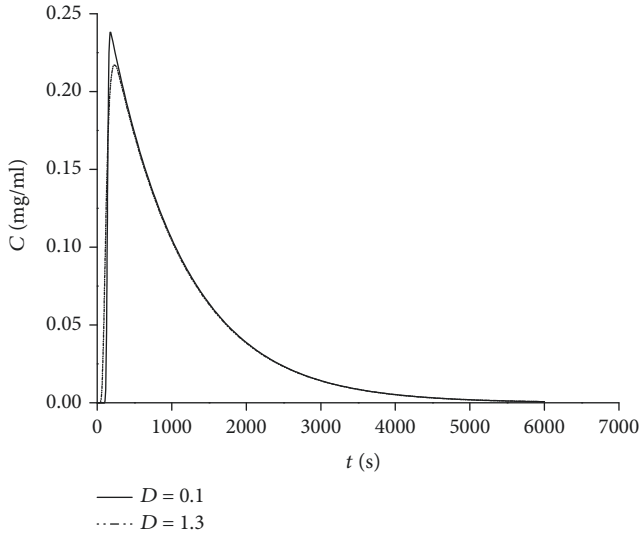


FIGURE 3: Relationship between particle concentration and time for two dispersion coefficients, using parameters given in Table 2.

TABLE 2: Model parameters used for simulations shown in Figure 3.

k_{dep} (s^{-1})	x (cm)	u (cm/s)	C_0 (mg/ml)	α' (s^{-1})
0.01	50	0.36	1	0.001

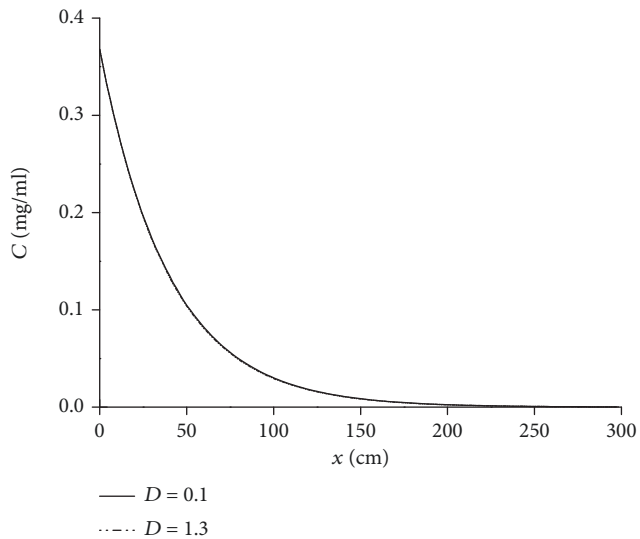


FIGURE 4: Relationship between particle concentration and distance for two dispersion coefficients, using parameters given in Table 3.

TABLE 3: Model parameters for simulations shown in Figure 4.

k_{dep} (s^{-1})	t (s)	u (cm/s)	C_0 (mg/ml)	α' (s^{-1})
0.01	1000	0.36	1	0.001

distance for the same four deposition coefficients using the parameters given in Table 5.

Figure 5 shows that the particle concentration rapidly peaked with increasing time, then gradually decreased to

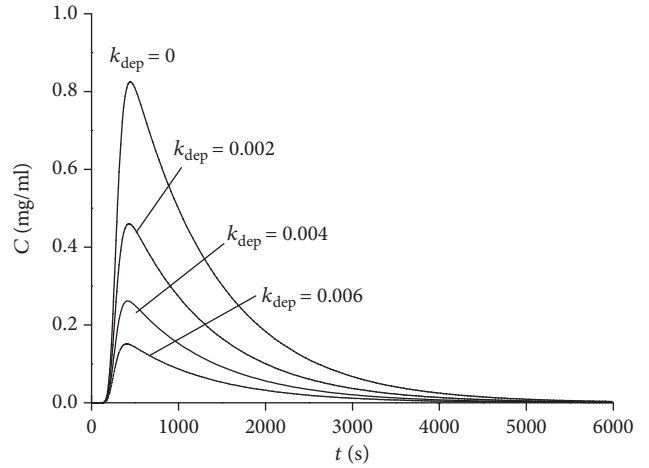


FIGURE 5: Relationship between particle concentration and time for four deposition rate coefficients, using parameters given in Table 4.

TABLE 4: Model parameters for simulations shown in Figure 5.

x (cm)	D (cm^2/s)	u (cm/s)	C_0 (mg/ml)	α' (s^{-1})
100	1	0.36	1	0.001

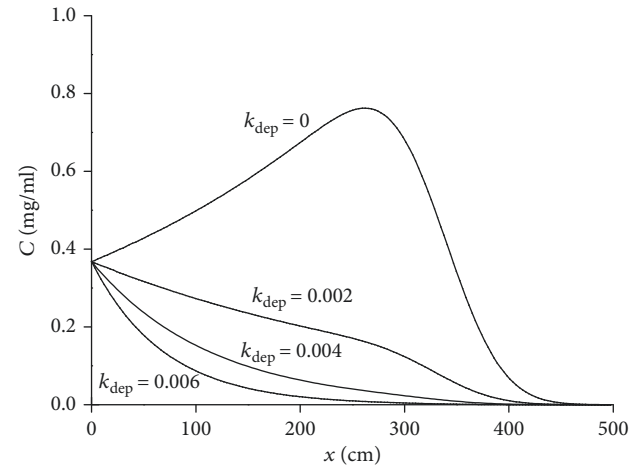


FIGURE 6: Relationship between particle concentration and distance for four deposition rate coefficients, using parameters given in Table 5.

TABLE 5: Model parameters for simulations shown in Figure 6.

t (s)	D (cm^2/s)	u (cm/s)	C_0 (mg/ml)	α' (s^{-1})
1000	1	0.36	1	0.001

zero. The peak value gradually decreased with increasing deposition coefficient, showing that this has a very important influence on particle transportation. Figure 6 shows that when the deposition coefficient was zero, the particle concentration gradually increased from about 0.35 to the peak with increasing distance, then decreased to zero. When the deposition coefficients were 0.004 and 0.006, the particle concentration decreased from 0.35 to zero with increasing distance.

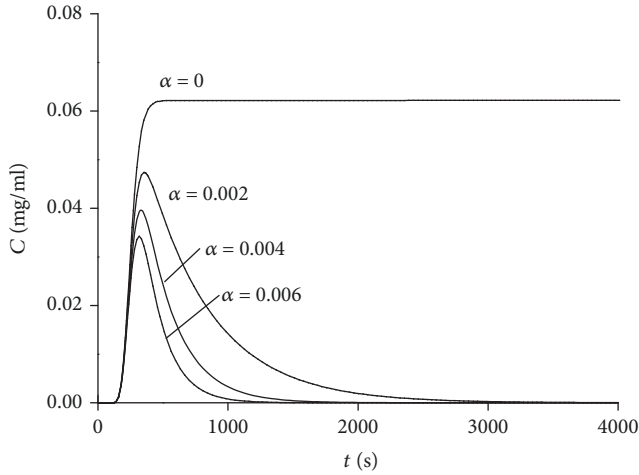


FIGURE 7: Relationship between particle concentration and time for four decay factors, using parameters given in Table 6.

Furthermore, when the deposition coefficient was 0.002, the particle concentration showed a transition period between deposition coefficients of 0 and 0.004. Overall, the particle concentration decreased with increasing deposition coefficient, showing that this has a great influence on the shape of such curves.

Figure 7 shows the relationship between particle concentration and time for four decay coefficients predicted by equation (18) using the parameters given in Table 6. Figure 8 shows the relationship between particle concentration and distance for the same decay coefficients using the parameters given in Table 7.

Figure 7 shows that when the decay coefficient was zero, the particle concentration peaked rapidly, then did not change further. When the decay coefficient was greater than zero, the concentration peaked rapidly, then gradually decreased to zero over time. In addition, the peak value of the particle concentration decreased with increasing decay coefficient. Figure 8 shows that the particle concentration decreased to zero with increasing distance and also decreased with increasing decay coefficient. Overall, the decay coefficient has a significant effect on particle transport.

4. Conclusion

We developed an analytical solution for a corrected convection-dispersion model that takes into account the effect of dispersion on deposition kinetics with regard to the particle concentration decay type. The rationality and correctness of the solution were verified using the time, distance, deposition coefficient, diffusion coefficient, and decay coefficient. The main conclusions are as follows:

- (1) Particle concentration increased from zero to the peak value with increasing time, then decreased to zero. However, particle concentration gradually reduced to zero with increasing transport distance

TABLE 6: Model parameters for simulations shown in Figure 7.

k_{dep} (s^{-1})	D (cm^2/s)	u (cm/s)	C_0 (mg/ml)	x (cm)
0.01	1	0.36	1	100

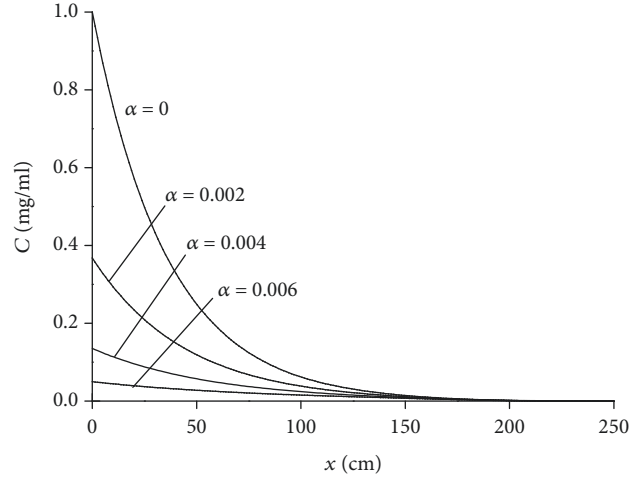


FIGURE 8: Relationship between particle concentration and distance for four decay factors, using parameters given in Table 7.

TABLE 7: Model parameters for simulations shown in Figure 8.

k_{dep} (s^{-1})	D (cm^2/s)	u (cm/s)	C_0 (mg/ml)	t (s)
0.01	1	0.36	1	500

- (2) Neglecting dispersion in the deposition kinetic equation can result in large errors in the relationship between particle concentration and time
- (3) With regard to time, the peak value of the particle concentration decreased gradually with increasing deposition coefficient, but the time corresponding to the peak value did not change
- (4) With regard to distance, the deposition coefficient affected the magnitude and distance of the peak value of the particle concentration
- (5) With regard to time, the peak value of the particle concentration decreased with increasing decay coefficient. With regard to distance, the peak value decreased with increasing decay coefficient

Data Availability

No data were used to support this study.

Disclosure

This paper was accepted for poster presentation at the 8th International Granulation Workshop, Sheffield, UK, 28–30 June 2017.

Conflicts of Interest

The authors declare that there is no conflict of interest regarding the publication of this paper.

Acknowledgments

This study was funded by the National Natural Science Foundation of China (NSFC; Grant No. 51778249 and 51778287) and the Promotion Program for Young and Middle-Aged Teacher in Science and Technology Research of Huaqiao University (Grant No. ZQN-PY513).

References

- [1] V. I. Malkovsky, V. A. Petrov, Y. P. Dikov, E. V. Alexandrova, Y. V. Bychkova, and L. S. Shulik, "Colloid-facilitated transport of uranium by groundwater at the U–Mo ore field in eastern Transbaikalia," *Environmental Earth Sciences*, vol. 73, no. 10, pp. 6145–6152, 2015.
- [2] S. Utsunomiya, A. B. Kersting, and R. C. Ewing, "Groundwater nanoparticles in the far-field at the Nevada Test Site: mechanism for radionuclide transport," *Environmental Science & Technology*, vol. 43, no. 5, pp. 1293–1298, 2009.
- [3] T. K. Sen and K. C. Khilar, "Review on subsurface colloids and colloid-associated contaminant transport in saturated porous media," *Advances in Colloid and Interface Science*, vol. 119, no. 2-3, pp. 71–96, 2006.
- [4] Q. Cai, C. W. W. Ng, X. Chen, L. Guo, and S. Su, "Effects of cementation on pore water pressure response during normal faulting in clay," *Géotechnique Letters*, vol. 8, no. 1, pp. 56–60, 2018.
- [5] N. Tufenkji, "Modeling microbial transport in porous media: traditional approaches and recent developments," *Advances in Water Resources*, vol. 30, no. 6-7, pp. 1455–1469, 2007.
- [6] A. Farrokhian Firouzi, M. Homaei, E. Klumpp, R. Kasteel, and W. Tappe, "Bacteria transport and retention in intact calcareous soil columns under saturated flow conditions," *Journal of Hydrology and Hydromechanics*, vol. 63, no. 2, pp. 102–109, 2015.
- [7] Z. You, A. Badalyan, Y. Yang, P. Bedrikovetsky, and M. Hand, "Fines migration in geothermal reservoirs: laboratory and mathematical modelling," *Geothermics*, vol. 77, pp. 344–367, 2019.
- [8] P. Bedrikovetsky, Z. You, A. Badalyan, Y. Osipov, and L. Kuzmina, "Analytical model for straining-dominant large-retention depth filtration," *Chemical Engineering Journal*, vol. 330, pp. 1148–1159, 2017.
- [9] Y. Yang, F. D. Siqueira, A. S. L. Vaz, Z. You, and P. Bedrikovetsky, "Slow migration of detached fine particles over rock surface in porous media," *Journal of Natural Gas Science and Engineering*, vol. 34, pp. 1159–1173, 2016.
- [10] G. E. Walshe, L. Pang, M. Flury, M. E. Close, and M. Flintoft, "Effects of pH, ionic strength, dissolved organic matter, and flow rate on the co-transport of MS2 bacteriophages with kaolinite in gravel aquifer media," *Water Research*, vol. 44, no. 4, pp. 1255–1269, 2010.
- [11] C. Yu, H. Wang, D. Fang, J. Ma, X. Cai, and X. Yu, "Semi-analytical solution to one-dimensional advective-dispersive-reactive transport equation using homotopy analysis method," *Journal of Hydrology*, vol. 565, pp. 422–428, 2018.
- [12] Z. Li and L. Zhou, "Cadmium transport mediated by soil colloid and dissolved organic matter: a field study," *Journal of Environmental Sciences*, vol. 22, no. 1, pp. 106–115, 2010.
- [13] N. Natarajan and G. S. Kumar, "Spatial moment analysis of colloid facilitated radionuclide transport in a coupled fracture-matrix system," *International Journal of Energy and Environment*, vol. 2, no. 3, pp. 491–504, 2011.
- [14] J. E. Altoé F., P. Bedrikovetsky, A. G. Siqueira, A. L. S. de Souza, and F. S. Shecira, "Correction of basic equations for deep bed filtration with dispersion," *Journal of Petroleum Science and Engineering*, vol. 51, no. 1-2, pp. 68–84, 2006.
- [15] J. S. Pérez Guerrero, E. M. Pontedeiro, M. T. van Genuchten, and T. H. Skaggs, "Analytical solutions of the one-dimensional advection–dispersion solute transport equation subject to time-dependent boundary conditions," *Chemical Engineering Journal*, vol. 221, pp. 487–491, 2013.
- [16] L. W. Lake, *Enhanced Oil Recovery*, Prentice Hall, Englewood Cliffs, 1989.
- [17] J. L. Jensen, L. W. Lake, P. W. M. Corbett, and D. J. Goggin, *Statistics for Petroleum Engineers and Geoscientists*, Prentice Hall PTR, New Jersey, 1997.
- [18] H. S. Carslaw and J. D. Jaeger, *Conduction of Heat in Solids*, Oxford University Press, London, 2nd edition, 1959.
- [19] M. Abramowitz and I. A. Stegun, *Handbook of Mathematical Functions with Formulas, Graphs, and Mathematical Tables. National Bureau of Standards Applied Mathematics Series 55*, John Wiley and Sons, New York, 10th edition, 1972.
- [20] H. Jin, S. Yu, S. Zhou, and J. Xiao, "Research on mechanics of longitudinal joint in shield tunnel by the nonlinear spring equivalent method," *KSCE Journal of Civil Engineering*, vol. 23, no. 2, pp. 902–913, 2019.
- [21] Q. P. Cai and C. W. W. Ng, "Analytical approach for estimating ground deformation profile induced by normal faulting in undrained clay," *Canadian Geotechnical Journal*, vol. 50, no. 4, pp. 413–422, 2013.
- [22] N. Tufenkji and M. Elimelech, "Deviation from the classical colloid filtration theory in the presence of repulsive DLVO interactions," *Langmuir*, vol. 20, no. 25, pp. 10818–10828, 2004.
- [23] B. E. Logan, D. G. Jewett, R. G. Arnold, E. J. Bouwer, and C. R. O'Melia, "Clarification of clean-bed filtration models," *Journal of Environmental Engineering*, vol. 121, no. 12, pp. 869–873, 1995.



Hindawi

Submit your manuscripts at
www.hindawi.com

